Neuroscience 130 (2005) 475–484

LOCALIZATION AND DEVELOPMENTAL EXPRESSION OF BK CHANNELS IN MAMMALIAN COCHLEAR HAIR CELLS

A. HAFIDI,* M. BEURG AND D. DULON*

Laboratoire de Biologie Cellulaire et Moléculaire de l'Audition, EA 3665, Université de Bordeaux 2, Laboratoire de Biologie Cellulaire et Moléculaire de l'Audition, CHU Hôpital Pellegrin, 33076 Bordeaux, France

Abstract—The expression of *Slo* channels (α subunits of BK channels) was investigated in the developing mouse cochlea using a polyclonal antibody against the C-terminal part of the protein (residues 1098–1196). The first BK channel immunoreactivity was observed in the cochlea at E18, where it was localized within the cytoplasm of cells lining the area of the organ of Corti and the spiral ganglion. There was an increase of immunoreactivity in all cells bordering the scala media (supporting and hair cells of the organ of Corti, the stria vascularis and the Reissner's membrane) in the following stages (postnatal day [P] 0 and P6). From P12 to adult, a strong membranous labeling, increasing with age, appeared in inner hair cells. The distribution of BK channels was mainly observed as dense elongated plaques localized in the lateral membrane below the cuticular plate. In addition, a more discrete immunolabeling for BK channels, as punctuated dots, was observed in the synaptic area of inner hair cells. This dual localization of BK channels within inner hair cells was confirmed by a different technique using a fluorescently labeled high-affinity ligand of these channels: IbTX-D19C-Alexa488. We demonstrated under patch clamp experiments that this fluorescent toxin conserved its native property, i.e. to reversibly inhibit BK currents in isolated inner hair cells. The fluorescent toxin, both in living or fixed tissues, also showed a preferential binding to mature inner hair cells with a similar subcellular distribution described above using immunocytochemical technique. Overall, our present results confirm the appearance of membranous BK channels around P12 in mouse inner hair cells, an age at which the auditory system becomes functional. The expression of BK channels in mature inner hair cells, near the site of mechanical-transduction, might serve to limit receptor potential attenuation due to the space constant, and thus permitting these sensory cells to function as fast and sensitive transducers.

Key words: hearing, cochlea, hair cells, potassium channels, calcium, iberiotoxin.

Large Ca^{2+}-activated K^+ channels, named BK or maxi-K channels, display a high unitary conductance (ranging from 75 to 250 pS), are activated by both membrane depolarization and intracellular Ca^{2+}, and are blocked by scorpion peptidyl toxins such as charybdotoxin and iberiotoxin (IbTX; for review see Vergara et al., 1998). These channels are composed of two structurally distinct subunits, α and β. The α subunits which form the main core of the BK channel are the product of a single *Slo* gene originally described in *Drosophila* (Atkinson et al., 1991).

BK channels are known to play a prominent role in the hair cell function of lower vertebrates such as amphibians, reptiles and avians (for review see Fettiplace and Fuchs, 1999). In these non-mammalian hair cells, BK channels are colocalized with Ca^{2+} channels at sites of transmitter release, the hair cell's pre-synaptic active zones (Roberts et al., 1990; Issa and Hudspeth, 1994). These BK channels are believed to regulate neurotransmitter release coupled to the calcium current at the lower vertebrate hair cell's active zone as at the nerve–muscle synapse (Robitaille et al., 1993; Pattillo et al., 2001). Remarkably, in electrically tuned hair cells, the number and the kinetic properties of BK channels (*Slo* splice variants) determine the resonant frequency of each hair cell along the basilar papilla (Rosenblatt et al., 1997; Navaratnam et al., 1997; Jones et al., 1999; Ramanathan et al., 1999). Electrical resonance is well known to act as an electrical filter maximizing the hair cell response at a specific sound frequency (Crawford and Fettiplace, 1981).

By contrast, the role of BK channels in mammalian cochlea hair cells remains more obscure since these hair cells do not display electrical resonance. Calcium-activated K^+ conductance has been described in both outer hair cells (OHC; Housley and Ashmore, 1992) and inner hair cells (IHC; Dulon et al., 1995; Kros et al., 1998; Oliver et al., 2003; Skinner et al., 2003). More recently, mRNA *Slo* expression has been shown in these hair cells and in particular in IHCs (Skinner et al., 2003; Langer et al., 2003). It has also been demonstrated with immunochemistry that adult guinea-pig IHCs express *Slo* proteins (Skinner et al., 2003). These *Slo* channels are believed to underlie the fast IbTX-sensitive K^+ conductance (IK_f) described in IHCs (Kros et al., 1998; Jagger and Ashmore, 1999; Skinner et al., 2003). In developing mouse IHCs, the expression of IK_f was shown to first appear at the onset of hearing around postnatal day (P) 12. The appearance of this fast BK current was shown to coincide with the loss of spontaneous action potentials, transforming mature mammalian IHCs into high-frequency signal transducers (Kros et al., 1998; Marcotti et al., 2003). The aim of the present study is to characterize the developmental expression of the *Slo* protein in the mouse cochlea and to determine

*Corresponding authors. Tel: +33-5-5624-2047; fax: +33-5-5696-2984.
E-mail addresses: didier.dulon@bordeaux.inserm.fr (D. Dulon); aziz.hafidi@univ-bpclermont.fr (A. Hafidi).

Abbreviations: DPBS, Dulbecco's phosphate buffer saline; E, embryonic stage; IbTX, iberiotoxin; IHC, inner hair cell; IK_f, IbTX-sensitive K^+ conductance; OHC, outer hair cell; P, postnatal; PBS, phosphate buffer saline.

0306-4522/05$30.00+0.00 © 2004 IBRO. Published by Elsevier Ltd. All rights reserved.
doi:10.1016/j.neuroscience.2004.09.038

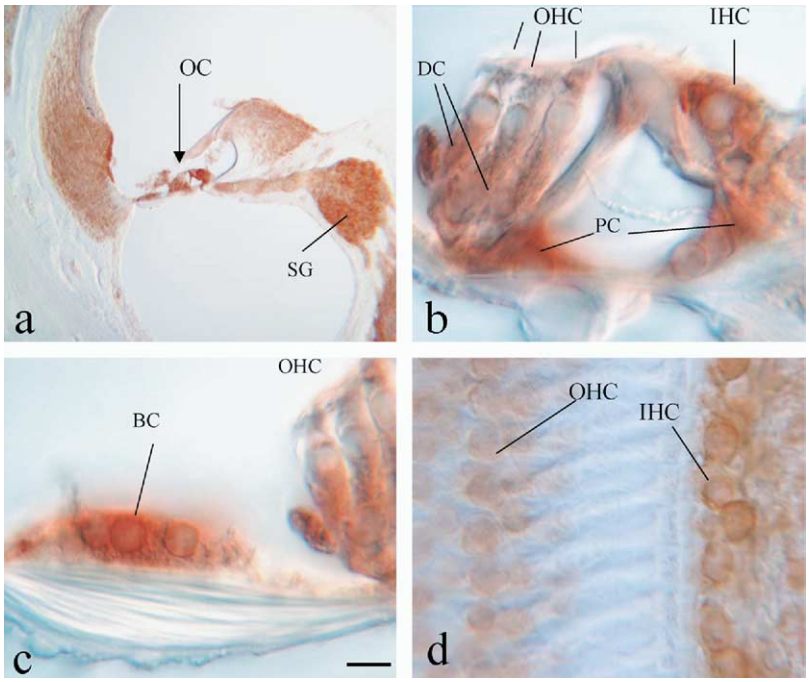

Fig. 1. Immunolocalization of the *Slo*-encoded proteins in the adult mouse cochlea. (a) At low magnification, the labeling was mainly observed in the organ of Corti, the spiral ganglion (SG), and the spiral prominence of the stria vascularis. (b) At high magnification of the organ of Corti, an intense labeling was observed in IHC and supporting cells, particularly the Deiters cells (DC) and the pillar cells (PC), while comparatively a weak labeling is present in the OHC. (c) High magnification of the outer lateral edge of the organ of Corti showing the labeling of the Böttcher cells (BC) located above the basilar membrane. (d) Surface preparation of the organ of Corti showing a more intense labeling within the IHCs compared with the OHCs. In C, scale bar=100 μm in A; 10 μm in B–D.

whether its expression coincided with the appearance of IK_f in mouse IHCs.

EXPERIMENTAL PROCEDURES

Immunohistochemistry

C57BL/6J mice at embryonic stages (E) 15–16 and 18, P0, P6, P12, P15 and adult were used for the present study. Minimums of five animals were used per stage. Mice were killed by cervical dislocation (adult) and/or were then decapitated. Animals were deeply anaesthetized before being killed and their handling throughout these experiments was performed with authorisation of the French Ministry of Agriculture and in accordance with EEC regulations. All efforts were made to minimize the number of animals used and their suffering. Cochleae were removed and placed immediately in a fresh solution of 4% paraformaldehyde in 0.1 M phosphate buffer. Cochleae were fixed 6 h to overnight at 4 °C in paraformaldehyde solution. Cochleae of adult, P6 and P12 mice were decalcified in 10% EDTA and washed in 01 M phosphate buffer saline (PBS) solution before cryostat or vibratome sectioning and surface preparation treatment. For cryostat sections, cochleae were put in a gradient of sucrose 10% (2 h), 20% (2 h) and 30% overnight. Cochleae were embedded in OCT medium and were frozen at −20 °C. Sections were collected free-floated in a PBS. At least 50 cochlear sections were mounted and observed for each developmental stage.

Immunohistochemistry was studied using cochlear vibratome sections (20 μm) as described previously (Hafidi, 1998). After decalcification, cochleae were embedded in a 4% agar solution. They were then sliced on a vibratome. Free-floating sections were treated for the immunohistochemistry as described below. After the stop of the DAB reaction, the sections were postfixed in a 1% OSO_4 solution, alcohol dehydrated, and embedded in epon 812 resin (Sigma Chemical). Semi-thin sections (1 μm) were obtained using the LKB ultramicrotome (LKB, Bromma, Sweden). Some sections were counterstained using a 1% Toluidine Blue solution before being observed at the light microscope.

For surface preparation of the organ of Corti, mice cochleae were dissected as described previously (Hafidi, 1998). Briefly, fixed cochleae were cut in to three pieces (base, middle-base and apex). The tectorial, Reissner and stria vascularis membranes were removed. Each remaining coil contained the organ of Corti, the spiral ligament and sometime the spiral ganglion. Cochlear coils were put in a 1% Triton X-100 solution (45 min), and washed several times in PBS.

Immunolocalization of Slo channels was carried out on cochlea sections and surface preparations of the organ of Corti using a specific polyclonal antibody (Alomone Laboratories). This primary antibody, raised in rabbit against the C-terminal part (residues 1098–1196) of mouse Slo a subunit, was used at 1:200 dilution. Samples were then washed, and incubated in biotinylated anti-rabbit secondary at dilution 1:200 (Sigma) for 2.5 h or fluorescein-conjugated secondary antibody for immunofluorescence. For peroxidase immunostaining, the signal was amplified with an avidin–biotin–horseradish peroxidase procedure (Vector Laboratory), and visualized using diaminobenzidine as the chromogen. Sections were rinsed, placed on subbed slides, dehydrated, cleared, and mounted for microscopic observation. Negative controls were carried out by the omission of the primary antibody and replacing it with PBS or by the use of a pre-adsorbed antiserum with its antigenic peptide (Alomone Laboratories). Light microscopy observations and image recordings were made with a high-resolution CCD camera system (Nikon DMX1200).

IHC preparation and whole-cell patch clamp recordings

IHCs were isolated from mouse or rat cochleae at P18–P25 as previously described (Dulon et al., 1995; Skinner et al., 2003). The two turns of the organ of Corti were removed from the bony shell of the cochlea and placed in Dulbecco's PBS (DPBS; Sigma). The organ of Corti, freed from the bony cochlea, was briefly incubated for 10 min in a 50 μl drop of DPBS containing trypsin at a final concentration of 0.5 mg/ml (Sigma). The organ of Corti segments were transferred to a 100 μl drop of DPBS placed in the center of a 30 mm Petri dish. The cells were then mechanically dissociated with gentle influx and efflux with a Gilson micropipette (Gilson, France), and left to settle for 30 min. The dish was then filled with 3–4 ml of DPBS. IHCs were recorded under voltage clamp configuration with electrodes pulled from borosilicate glass capillaries (GC150TF-10; Clark Electromedical, UK), on a Sachs-Flaming horizontal electrode puller (Sutter Instruments, USA). Recording electrodes were backfilled with the following internal solution containing in mM: KCl 158, $MgCl_2$ 2, EGTA 1.1, HEPES 5, KOH 3.5, pH 7.20. Patch-clamp recordings were performed as previously described in detail (Blanchet et al., 1996) by means of an Axopatch-200B amplifier (Axon Instruments, Foster City, CA, USA). pClamp 8.0 software (Axon Instruments) was used for data collection and analysis. Voltage errors attributable to uncompensated series resistance and liquid junction potential were corrected during data analysis (Blanchet et al., 1996). All experiments were performed at room temperature (20–22 °C).

Direct fluorescent labeling of BK channels with IbTX-D19C-Alexa488

The fluorescent derivative of IbTX, IbTX-D19C-Alexa488, was kindly provided by Dr Hans-Guenther Knaus (Innsbruck, Austria). This fluorescent toxin was applied to living isolated hair cells at a concentration of 50 nM by a Picospritzer puffer system (Picospritzer II; General Valve, Fairfield, NJ, USA). Pipettes for the Picospritzer system were pulled in a similar fashion to the recording patch-clamp pipettes and were placed at 20–40 μm from the cells. The pressure of the perfusion system was set low enough to avoid any mechanical disturbance of the cell during current recording. Using this system, the toxin was applied for 15 s to the cell membrane. In the case of living explants of organ of Corti (in DPBS) or fixed cryosections of adult mouse cochleae (2 months), the fluorescent toxin was incubated at 50 nM for 30 min prior to observation with fluorescence microscopy.

RESULTS

Distribution of BK channels in the adult mouse cochlea

Immunoreactivity of *Slo* channels was observed in various structures of the mature cochlea. Mid to strong expression was noted in the spiral ligament and in the surface cells of the spiral prominence (Fig. 1a). A strong immunoreactivity was also observed in Böttcher cells located on the pars pectinata of the basilar membrane and in Claudius cells (Fig. 1a–c). In the organ of Corti, a strong expression was observed in IHCs (Fig. 1a, b). We could identify no evidence for a gradient of differential expression along the length of the cochlear partition for IHC from the base to apical regions. A significant labeling was also observed in supporting cells of the organ of Corti, in particular Deiters cells and pillar cells. Above the Deiters cells, the OHCs displayed a moderate labeling compare with IHCs, with again no difference along the cochlear partition and between the three OHC rows (Fig. 1c, d). The somas of spiral ganglion neurons were strongly labeled while their inner radial fibers, which innervate the IHCs, remained essentially unlabeled (Fig. 1a).

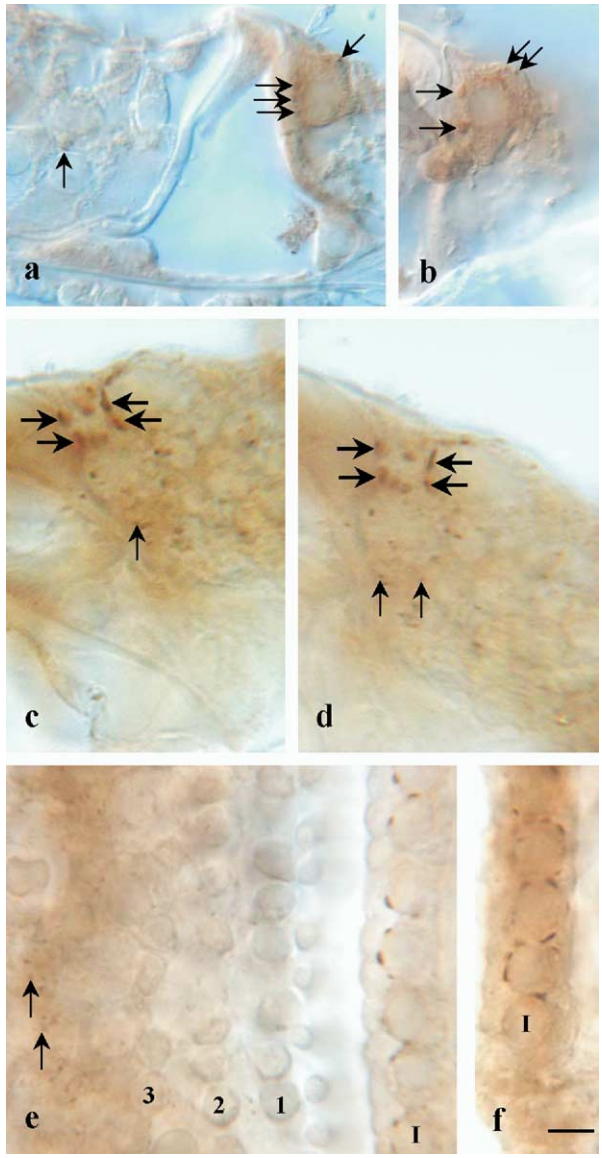

Fig. 2. Immunolocalization of *Slo*-encoded proteins in IHCs. (a–d) Cross-sections of the organ of Corti in the region of the IHCs shows a strong labeling at the apical neck region (below the cuticular plate, thick arrows) and punctuated labeling at their synaptic basal region (thin arrows). Dot-like labeling (a) is observed at the base of OHC (arrow). (e, f) Surface preparations of the organ of Corti (I for IHCs and 1, 2, 3 for the three rows of OHCs) shows a section view of these plaques of BK channels at the apical region of the IHCs. Again only dot-like labeling is observed at the base of OHCs (e). Scale bar = 10 μm.

A similar expression of *Slo* protein was observed in surface preparations of the adult organ of Corti. A strong labeling was noted in the IHCs, in the interdental cells of the spiral limbus and in spiral ganglion neurons, while OHCs were lightly labeled (Fig. 1d; Fig. 2e, f). The IHC

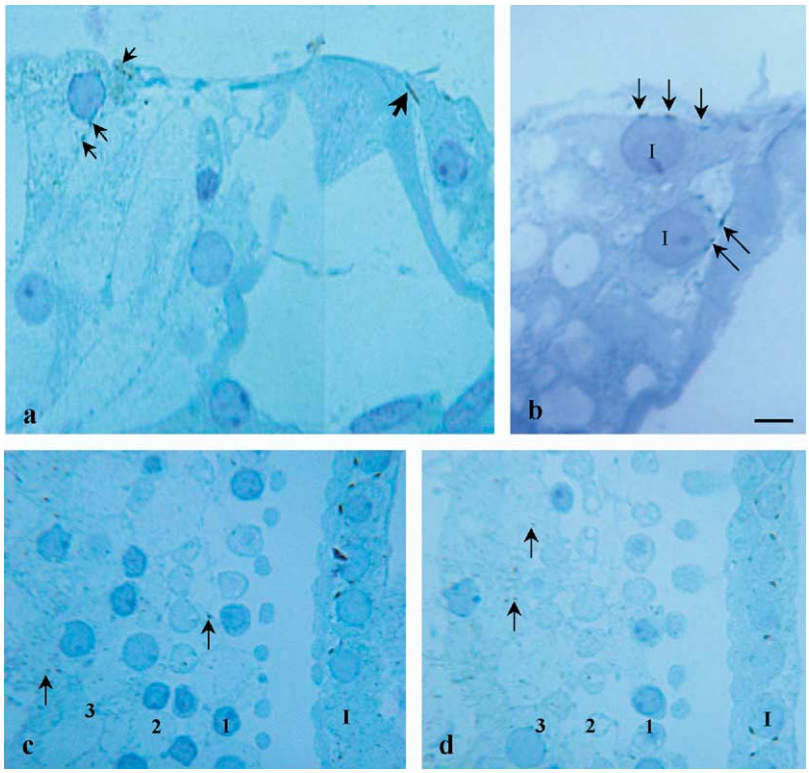

Fig. 3. Immunolocalization of *Slo* BK channels in semi-thin section of the organ of Corti. Within the organ of Corti, the labeling is observed as dots (thin arrows) in Hensen's cells, while plaque staining (thick arrow) is present at the apical pole of the IHC (a). In a cross-section of the IHC (b) the plaque staining is observed along the lateral membrane from the nucleus level to the cuticular area. In this section two IHCs are represented. In a transverse sections of the organ of Corti (c, d) a similar staining is observed, with a dot-like staining present at the base of OHCs (arrows) and plaque labeling located surrounding the neck of the IHCs. Scale bar=10 μm.

presented intense plaques labeling localized below the cuticular plate. This staining was confirmed in vibratome sections where plaque labeling was observed in IHCs in the lateral membrane below the cuticular plate (Figs. 1b and 2a–d). When the entire IHC was observed the labeling could be observed in plaques surrounding the apical pole of the cell. Such pattern of BK labeling was systematically observed in all cochlear sections and surface preparation of the organ of Corti.

The examination of semi-thin cross-sections, at high magnification, indicated a strong distribution of *Slo* BK channels in the apical portion of the IHCs. This labeling appears as independent plaques lying beneath the cuticular plate (Fig. 3). These dense plaques of *Slo* proteins appeared to be located at the plasma membrane, delimiting the cell contour in their apical portion below the cuticular plate, as shown in the surface preparations and semi-thin sections of the organ of Corti. In addition, below these plaques, a dot-like pattern of labeling of *Slo* channels was observed in the lower part of the IHCs. This punctuated basal labeling was lateralized to the surface membrane around and below the IHC nucleus, presumably where afferent fibers make synaptic contact. The number of dots per section of IHC ranged from four to seven with a mean diameter around 1 μm (Fig. 2). In OHCs, the level of *Slo* protein expression was much lower throughout the cell and was mainly observed at their basal portion, presumably at the pre-synaptic membrane facing the large efferent synapses (Fig. 2). In supporting cells of the organ of Corti such as Deiters cells and pillar cells, both cryosections, surface preparations and semithin sections indicated a diffuse labeling throughout the cell cytosol and there was no evidence for a strong expression of *Slo* channels in their plasma membrane (Figs. 1, 2, 3).

Direct labeling of BK channels with IbTX-D19C-Alexa488

To confirm the localization of BK channels in cochlear tissue, we used a high-affinity ligand and blocker of BK channels, IbTX. The toxin was tagged with a fluorescent molecule (Alexa488) in order to directly visualize its cellular binding sites. The modified toxin was first examined in patch clamp experiments, to verify that it conserved its inhibitory properties toward BK currents in isolated mature IHCs. As expected for the native toxin (Kros et al., 1998; Skinner et al., 2003), a 10 s application of 50 nM IbTX-Alexa488 to IHCs reversibly inhibited a fast component of the outward K^+ current (Fig. 4a, b). The labeled toxin largely inhibited the fast outward rectifying current as shown in the current-voltage curve (Fig. 4). Such current inhibition by IbTX-Alexa488 was observed in all six IHCs examined. Both the kinetics and amplitude of the IbTX-Alexa488 sensitive-currents resembled those observed

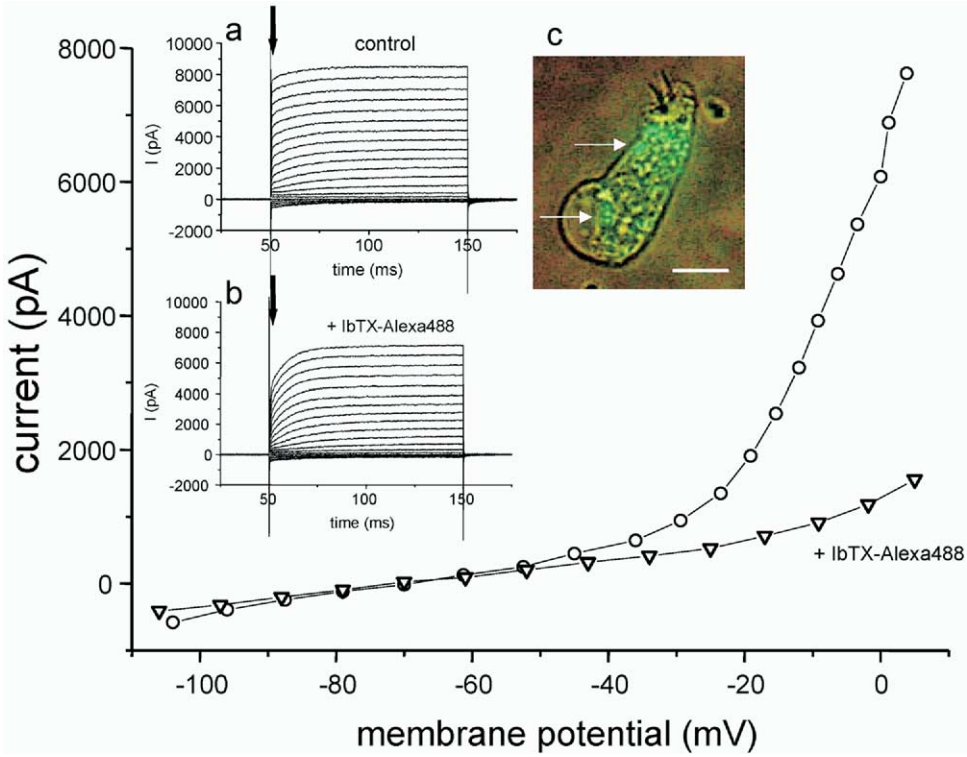

Fig. 4. IbTX-Alexa488 inhibits a fast outward current in isolated IHCs. The fast component of the whole cell outward current (a) was reduced in presence of 50 nM of IbTX-Alexa488 (b). The cell membrane potential was stepped in 10 mV increment from a holding potential of −70 mV. The amplitude of the fast outward current was measured at 2 ms as indicated by the vertical arrows. The current–voltage relationship measured (corrected from voltage drop across series resistance) showed a strong outward rectification near −50 mV that was drastically reduced by the fluorescent toxin. In c, is shown an example of isolated IHC viewed under fluorescence microscopy after labeling with 50 nM of IbTX-Alexa488. The white light illumination was set at a minimum to see the cell contour without blurring the Alexa488 fluorescence.

with the native unlabeled IbTX (Skinner et al., 2003). This observation indicated that the IbTX-Alexa488 conserved its binding properties to the BK channels of IHCs.

Under fluorescence microscopy, isolated IHCs exposed to a brief 10 s puff of IbTX-Alexa488 typically displayed a strong fluorescent labeling, consisting of elongated plaques running from the cuticular plate to the upper part of the nucleus (Figs. 4c, 5b). Such a fluorescent pattern was systematically observed in more than 25 IHCs isolated from either the base or the apex of different mouse cochleae. A similar pattern of labeling was additionally observed in IHCs isolated from other mammalian species such as adult rat and guinea-pig (data not shown). These fluorescent plaques were immediately visible after the 10 s application of the IbTX-Alexa488 (Fig. 5b2, b3) and they progressively disappeared after several minutes of washout or with an application of 1 μM of the native nonfluorescent IbTX (Fig. 5b4). These results indicated a reversible binding of the fluorescent toxin at specific targets on the plasma membrane of IHCs. Pre-incubating IHCs with the native nonfluorescent IbTX at a saturating concentration of 1 μM prior to puffing IbTX-Alexa 488 (50 nM) prevented the appearance of the fluorescent plaques in all IHCs tested (n=5). This again suggested that the native and the labeled IbTX compete at the same binding sites, presumably the *Slo* BK channels.

A similar fluorescent labeling of plaques below the cuticular surface of IHCs was also observed in fresh preparation of the organ of Corti *in vitro* (Fig. 5a). The dense apical plaques of *Slo* channels in IHCs, labeled with IbTX-Alexa488, were also revealed in cross-sections of fixed cochleae (Fig. 4c).

In addition to the observation of plaques of BK channels at the apical surface, there was also a sparse dot-like labeling in the more basal synaptic area of the IHCs (Fig. 4c and Fig. 5a). These results suggested that there was an additional expression of *Slo* channels in the presynaptic zones of IHCs, and this is in agreement with the immunohistochemical results described in the previous paragraphs (Fig. 2). In sections of fixed adult mouse cochleae, IbTX-Alexa488 also strongly labeled the dark cells of the stria vascularis. The BK channels appeared to be located at the plasma membrane, facing the endolymphatic compartment, in these cells.

There was no apparent labeling of the organ of Corti supporting cells with the fluorescent toxin suggesting that the *Slo* immunolabeling observed in these structures (Fig. 1) was intracellular, and thus inaccessible to the toxin. This suggestion was reinforced by the absence of fluorescent labeling in isolated living Deiters cells directly exposed to IbTX-Alexa488 (representative of five Deiters cells; Fig. 6a). Isolated living OHCs from mature mice, rat or guinea-

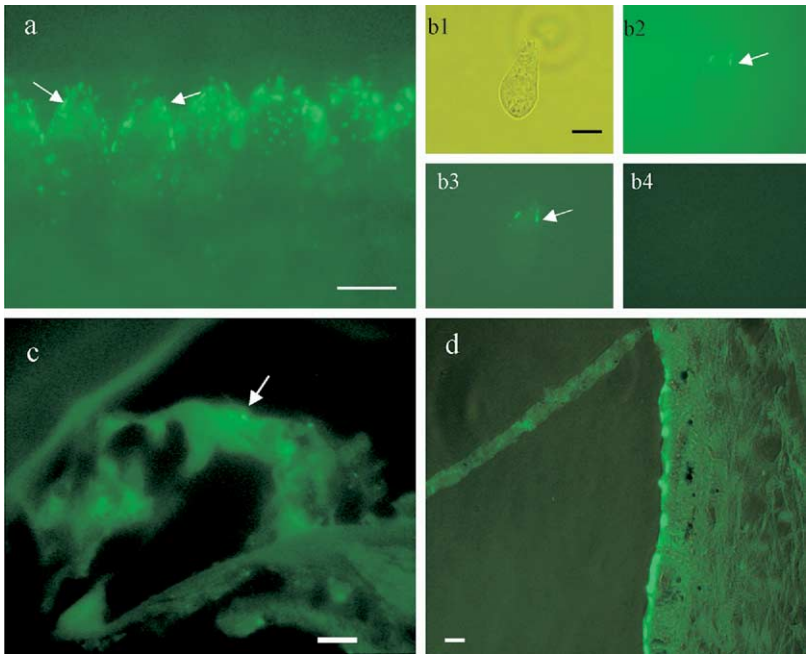

Fig. 5. Localization of BK channels with IbTX-Alexa488. (a) Fluorescent image in the area of the IHCs from a living piece of organ of Corti treated with 50 nM IbTX-Alexa488 for 30 min. Note the labeling of apical plaques below the cuticular plate of the IHCs as indicated by the arrows. In absence of the fluorescent toxin, the organ of Corti did not show fluorescence (not shown). (b) Example of labeling with 50 nM IbTX-Alexa488 in an isolated living IHC. (b1) In bright field microscopy; (b2) the same IHC visualized under fluorescence immediately at the end of the 10 s puff application of the fluorescent IbTX. (b3) The same IHC under fluorescence microscopy 30 s after the end of the puff (note the decrease of the fluorescent background and the labeling of the plaques below the cuticular plate); (b4) the same cell under fluorescence microscopy after application of 1 μM of the native nonfluorescent IbTX. (c) Example of a frozen cross-section from an adult cochlea treated with IbTX-Alexa488. Note the labeling of the plaque below the cuticular plate of the IHC (arrow). (d) Cross-section in the region of the stria vascularis showed a strong labeling of the dark cells by the fluorescent toxin. The horizontal scale bars=10 μm.

pig cochleae were also exposed to the fluorescent toxin in order to directly visualize *Slo* BK channels at the plasma membrane (Fig. 6b, c). We never observed a fluorescent labeling of plaques in the sub-cuticular region of isolated OHCs that resembled the pattern observed in IHCs ($n>50$ OHCs isolated from rat, mice or guinea-pig cochlea). A strong membranous labeling was, however, observed in the synaptic zone of basal OHCs (10 out 50 cells) where efferent cholinergic nerve endings contact these cells (Fig. 5c). These results suggested that, beside SK channels, BK channels may also participate in the cholinergic hyperpolarization response of OHCs.

Developmental expression of BK channels

The expression of *Slo* proteins was now investigated in the developing mouse cochlea using immunocytochemistry. At E15–E16, the BK immunoreaction in all cochlear tissues was very weak or nonexistent (Fig. 7a, b). The supporting and hair cells of the organ of Corti were not labeled (Fig. 7a, b), in a similar fashion to control immunoreactions realized with preabsorbed antibodies (Fig. 7m). These results suggested that the expression level of BK channels was very low or absent at this early stage of embryonic development. At E18, the overall immunoreaction in the cochlea increased, particularly in all cell structures facing the scala media of the cochlea. Supporting and hair cells showed intracytoplasmic labeling (Fig. 7c, d). At P0, the immunoreaction again increased in all cell structure lining the scala media: e.g. the stria vascularis, Reissner's membrane, the upper surface of the spiral limbus (interdental cells and inner spiral sulcus), and the organ of Corti (Fig. 7e, f). There was also a strong immunolabeling in spiral ganglion neurons. At P6, there was again a strong immunoreaction in the cochlea similar to P0. In the organ of Corti, both IHC and OHCs were again clearly labeled (Fig. 7g, h). At all these developmental stages, from E18 to P6, the immunostaining of the *Slo* proteins was restricted to the cytosol of supporting and sensory hair cells, suggesting that the *Slo* proteins were not yet targeted at specific sites on the plasma membrane. Supporting that assumption was that the absence of any fluorescent labeling of the organ of Corti at P6, when cochlea cross-sections were treated with IbTX-Alexa488 (data not shown). One possible explanation for the absence of IbTX-Alexa488 binding sites at P6 was that *Slo* proteins do not yet form membranous channel tetramers that would allow specific binding of the toxin at this early stage of development.

At P12–P15, the *Slo* immunoreaction in the organ of Corti showed a clear intensification and cellular restriction of the labeling to IHCs (Fig. 7i–l and Fig. 8). This stage corresponds to the onset of hearing in mouse and *Slo* proteins were concentrated at plaques below the cuticular plaques of IHCs in a similar fashion to mature cochleae. A dot-like pattern was also observed in the synaptic region of

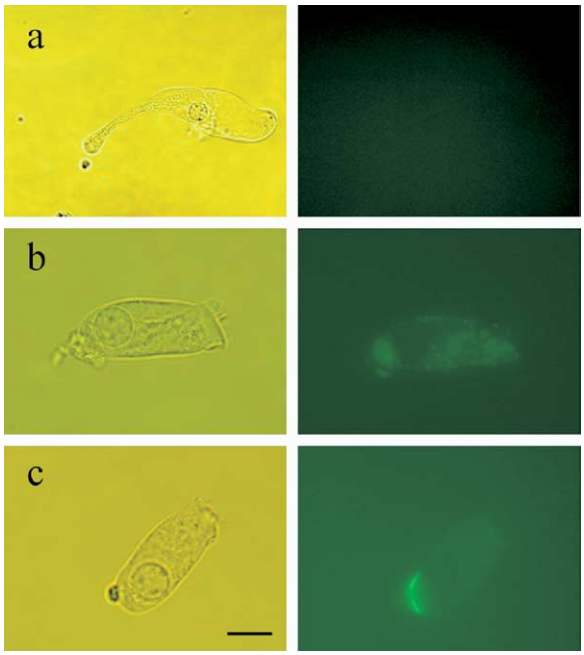

Fig. 6. Binding sites of IbTX-Alexa488 in freshly isolated living Deiters and OHCs of the organ of Corti. (a) In the left panel is shown an example of isolated Deiters cell visualized in bright field microscopy. In the right panel is shown the same cell under fluorescence microscopy 30 s after the application of the fluorescent toxin as in Fig. 5b3. Note the absence of fluorescent binding sites in these supporting cells. (b) In the left panel is shown an example of isolated living OHC in bright field microscopy and under fluorescence after the application of the fluorescent toxin in the right panel (note the absence of fluorescent binding sites). (c) In the left panel is shown an example of isolated OHC showing a strong membranous labeling with IbTX-Alexa488 (right panel). Note that the labeling was restricted to the basal synaptic area of the OHC, as a cup-shaped form, where cholinergic efferent fibers make large synaptic contacts.

IHCs. In OHCs, there was only a light labeling, likely corresponding to a diffuse cytoplasmic localization of aBK proteins.

DISCUSSION

Our study clearly shows that mature IHCs of the mouse cochlea strongly express the *Slo*-encoded α-subunit protein, known to constitute when assembled in tetramers functional BK channels (Atkinson et al., 1991). These results are in agreement with recent studies showing that adult rat IHCs express *Slo* transcripts mRNA (Brandle et al., 2001; Skinner et al., 2003; Langer et al., 2003). They also fit well with recent studies showing strong immunolabeling of BK channels in mature guinea-pig or mouse IHCs (Skinner et al., 2003; Rüttiger et al., 2004). The BK channels are believed to underlie IK_f, a fast potassium current that largely reduces the time constant of the receptor potential in adult IHCs (Kros and Crawford 1990; Kros et al., 1998; Skinner et al., 2003). The present study further demonstrated that the *Slo* immunoreaction in IHCs was largely restricted to dense membranous plaques below the cuticular plates, but also in sparse locations at the basal synaptic area. This specific membranous location of BK channels was confirmed by using a specific fluorescent toxin that binds directly to BK channels. The IbTX-Alexa488 was indeed shown to rapidly and reversibly label apical plaques and basal dots in IHCs. This labeling was presumably located at the plasma membrane since the peptide toxin should rather be cell impermeable during our brief application in living cells. Moreover, the dense extrasynaptic plaques of BK channels in mature IHCs were located at the same apical region where α-1D (Hafidi and Dulon, 2004) and ryanodine receptors (RyR1; Beurg et al., 2003) were found. This is interesting, since these two calcium channels were recently demonstrated to regulate the activity of two types of BK currents in IHCs (Marcotti et al., 2004). This peculiar extrasynaptic distribution of BK channels and α-1D channels in IHCs was also reported by Waka et al. (2003). The immuno-localization of BK channels as punctuated dots at the basal synaptic region of IHCs suggested that these potassium channels are also located at the presynaptic zones as demonstrated in lower vertebrate hair cells (Roberts et al., 1990; Issa and Hudspeth, 1994; Fettiplace and Fuchs, 1999). It remains to be determined if these distinct locations for the BK channels (e.g. a large expression at apical extrasynaptic plaques and a more discrete dot-like expression at synaptic zones) are associated with the two types of BK currents described in mice IHCs by Marcotti et al. (2004).

The functional implications for such a dense distribution of BK channels at the neck of IHCs, and just below the cuticular plate and the stereocilia, are unknown. The BK channels of IHCs have very fast kinetics (Kros et al., 1998; Skinner et al., 2003) and their location below the cuticular plate would permit a more rapid repolarization during sound stimulation. An apical localization of BK channels would also more rapidly and efficiently extrude the K^+ ions entering the cell through the transducer channels. Interestingly, KCNQ4 channels are expressed at the same apical region of mice IHCs, and these channels would also contribute to K^+ ion extrusion and cell repolarization (Oliver et al., 2003).

During cochlear development, we found that *Slo* immunoreactivity was first identified at the E18 with an intracellular labeling in all cell structures lining the scala media. From P0 to P6, the *Slo* labeling clearly increased in supporting and hair cells of the organ of Corti, but again the immunoreactivity appeared localized within the cell cytoplasm, in agreement with the absence of fluorescent binding sites for IbTX-Alexa488. At these early stages of organ of Corti development, we believe that the cytoplasmic *Slo* proteins were not yet targeted and assembled as channel tetramers in the plasma membrane of supporting cells and hair cells. The absence of targeting or assembling proteins such as slob (slowpoke-binding protein) and slip-1 (*Slo*-interacting protein 1), known to regulate the cellular distributions of BK channels within cells (Schopperle et al., 1998; Xia et al., 1998), could, for example, explain the absence of membranous BK channels at the early developmental stages in IHCs.

We found that the expression of membranous *Slo* proteins occurs around P12 in the developing mice IHC, and this is about the same time that hearing onset occurs. These results are in good agreement with the appearance

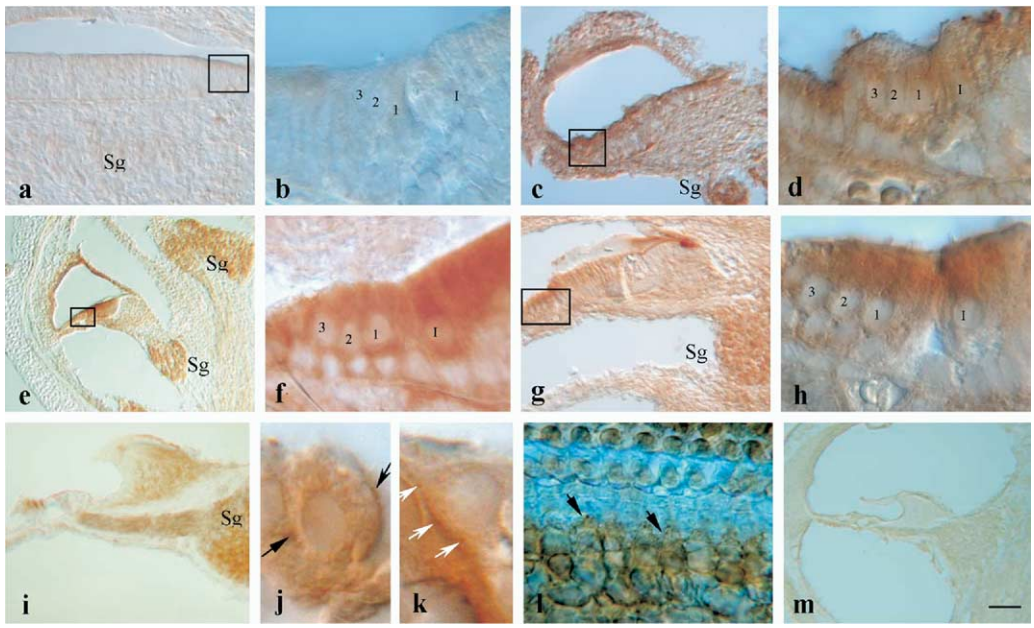

Fig. 7. Developmental expression of the *Slo* encoded protein in the mouse cochlea. Negative or background staining is observed in a cryostat cross-section of the cochlea at E16 (a, b). The first defined staining is observed in cross-section of the cochlea at E18 (c). The labeling is observed in cells lining the scala media, the spiral ganglion (Sg), and the organ of Corti (square). At high magnification of the organ of Corti (square in c), a cytoplasmic staining is present in both sensory hair cells and supporting cells (d). The labeling increases by the following stages P0 (e, f) and P6 (g, h) and was present in the same structures described previously. At P12, the same staining is observed (i); however, at high magnification of the IHCs (j, k), a plaque staining is present within the lateral cell membrane (arrows). The plaque staining at the IHC neck is also obtained in surface preparation of the organ of Corti at this stage (l). Negative staining is obtained in a control section using preadsorbed antibody (m). The scale bar=100 μm for a; 200 μm for c, e, g, i, and m; 10 μm in b, d, f, h, j, k, and l.

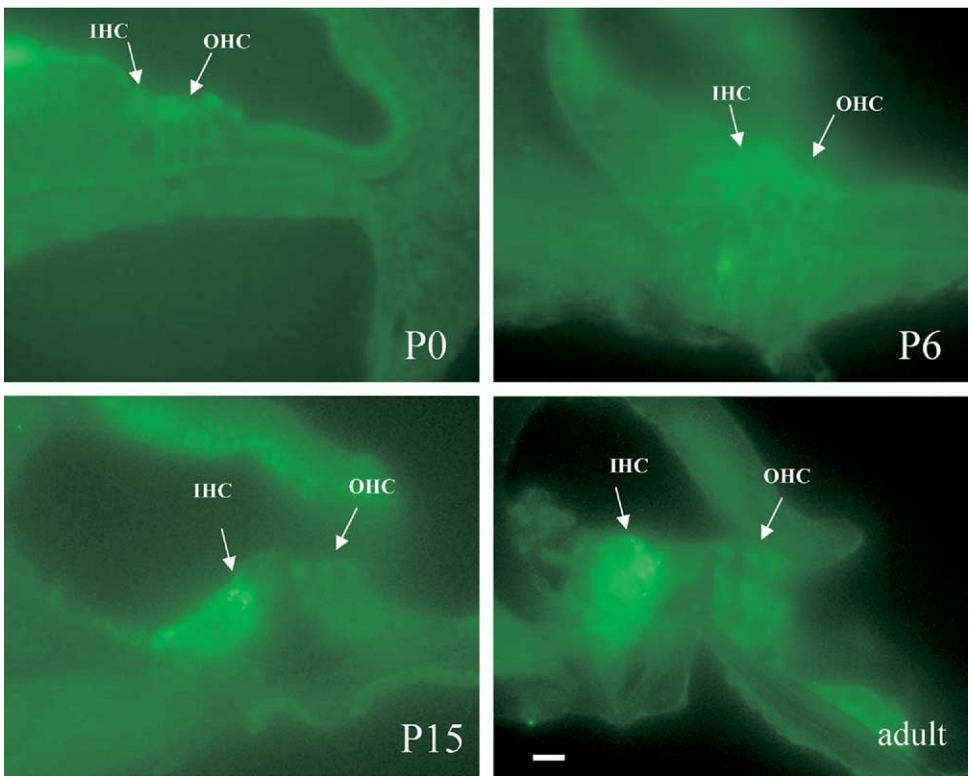

Fig. 8. Developmental expression of the *Slo*-encoded protein in the organ of Corti using a secondary antibody coupled to Alexa488. At P0 and P6 there was only a diffuse cytoplasmic labeling in the area of the hair cells of the organ of Corti. At P15 and adult, IHCs showed a strong apical plaque and dot-like labeling. The scale bar=10 μm.

of the fast potassium conductance $IK_{,f}$ in developing mice IHCs (Kros et al., 1998; Marcotti et al., 2003). It is also interesting to note that the membranous expression of BK channels between P11 and P14 in mouse IHCs develops at the same time as the afferent synapses and the full elaboration of the presynaptic complex (Sobkowicz, 1992).

Our study demonstrated that adult OHCs express BK channels in agreement with previous electrophysiological recordings (Housley et al., 1992; Nenov et al., 1997). In addition, the immunolabeling and the binding of IbTX-Alexa488 were consistently observed in short basal OHCs, and in their synaptic region where efferent cholinergic fibers make contact. These results suggested that BK channels could participate with SK channels in the cholinergic hyperpolarizing response of cochlear OHCs (Blanchet et al., 1996; Nenov et al., 1996; Dulon et al., 1998). Although we cannot completely exclude an involvement of BK channels in OHCs afferent transmission, the labeling pattern of BK channels, mostly observed at basal short OHCs with a cup-form shape at their base, suggested an implication in the efferent cholinergic stimulation.

In conclusion, we demonstrated for the first time a dual location of BK channels in mature IHCs: a large expression as membranous apical plaques below the transduction sites, and a punctuated expression in the synaptic area of the cell. Furthermore, we showed that the developmental appearance of BK channels at the plasma membrane of IHCs occur near P12–P15 at the onset of peripheral auditory function and the onset of hearing. While our manuscript was under revision, a study by Rüttiger et al. (2004) confirmed the localization of the αBK protein in the upper (supranuclear) part of IHCs and postsynaptically in OHCs in close apposition to synaptophysin-immunopositive efferents.

Acknowledgments—We are grateful to Professor James Saunders for his comments and English correction of the manuscript.

REFERENCES

Atkinson NS, Robertson GA, Ganetzky B (1991) A component of calcium-activated potassium channels by the *Drosophila Slo* locus. Science 253:551–555.

Beurg M, Skinner S, Aran JM, Dulon D (2003) Implication of ryanodine receptors in the process of cochlear amplification and neurotransmission: an in-vivo study. Abstract 1841 ARO 2003.

Blanchet C, Erostegui C, Sugasawa M, Dulon D (1996) Acetylcholine-induced potassium current of guinea-pig outer hair cells: its dependence on a calcium influx through nicotinic-like receptors. J Neurosci 16:2574–2584.

Brandle U, Frohnmayer S, Krieger T, Zenner HP, Ruppersberg JP, Maassen MM (2001) Expression of $Ca^{(2+)}$-activated $K^{(+)}$ channel subunits and splice variants in the rat cochlea. Hear Res 161:23–28.

Crawford AC, Fettiplace R (1981) An electrical tuning mechanism in turtle cochlear hair cells. J Physiol 312:377–412.

Dulon D, Sugasawa M, Blanchet C, Erostegui C (1995) Direct measurement of $Ca^{(2+)}$-activated K^+ currents in inner hair cells of the guinea-pig cochlea using photolabile Ca^{2+} chelators. Pflugers Arch 430:365–373.

Dulon D, Luo L, Zhang C, Ryan AF (1998) Expression of small-conductance calcium-activated potassium channels (SK) in outer hair cells of the rat cochlea. Eur J Neurosci 10:907–915.

Fettiplace R, Fuchs PA (1999) Mechanisms of hair cell tuning. Annu Rev Physiol 61:809–834.

Hafidi A (1998) Peripherin-like immunoreactivity in type II spiral ganglion cell body and projections. Brain Res 805:181–190.

Hafidi A, Dulon D (2004) Developmental expression of Ca(v)1.3 (alpha1D) calcium channels in the mouse inner ear. Dev Brain Res 150:167–175.

Housley GD, Ashmore JF (1992) Ionic currents of outer hair cells isolated from the guinea-pig cochlea. J Physiol 448:73–98.

Issa NP, Hudspeth AJ (1994) Clustering of Ca^{2+} channels and $Ca^{(2+)}$-activated K^+ channels at fluorescently labeled pre-synaptic active zones of hair cells. Proc Natl Acad Sci USA 91:7578–7582.

Jagger DJ, Ashmore JF (1999) The fast activating potassium current, (I(K,f), in guinea-pig inner hair cells is regulated by protein kinase A. Neurosci Lett 263:145–148.

Jones EM, Gray-Keller M, Fettiplace R (1999) The role of Ca^{2+}-activated K^+ channel spliced variants in the tonotopic organization of the turtle cochlea. J Physiol 518:653–656.

Kros CJ, Crawford AC (1990) Potassium currents in inner hair cells isolated from the guinea-pig cochlea. J Physiol 421:263–291.

Kros CJ, Ruppersberg JP, Rusch A (1998) Expression of a potassium current in inner hair cells during development of hearing in mice. Nature 394:281–284.

Langer P, Grunder S, Rusch A (2003) Expression of Ca^{2+}-activated BK channel mRNA and its splice variants in the rat cochlea. J Comp Neurol 455:198–209.

Marcotti W, Johnson SL, Holley MC, Kros CJ (2003) Developmental changes in the expression of potassium currents of embryonic, neonatal and mature mouse inner hair cells. J Physiol 548: 383–400.

Marcotti W, Johnson SL, Kros CJ (2004) Effects of intracellular stores and extracellular $Ca^{(2+)}$ on $Ca^{(2+)}$-activated $K^{(+)}$ currents in mature mouse inner hair cells. J Physiol 557 (Pt 2): 613–633.

Navaratnam DS, Bell TJ, Tu TD, Cohen EL, Oberholtzer JC (1997) Differential distribution of Ca^{2+}-activated K^+ channel splice variants among hair cells along the tonotopic axis of the chick cochlea. Neuron 19:1077–1085.

Nenov AP, Norris C, Bobbin RP (1996) Acetylcholine response in guinea pig outer hair cells: II. Activation of a small conductance $Ca^{(2+)}$-activated K^+ channel Hear Res 101:149–172.

Nenov AP, Norris C, Bobbin RP (1997) Outwardly rectifying currents in guinea pig outer hair cells. Hear Res 105:146–158.

Oliver D, Knipper M, Derst C, Fakler B (2003) Resting potential and submembrane calcium concentration of inner hair cells in the isolated mouse cochlea are set by KCNQ-type potassium channels. J Neurosci 23:2141–2149.

Pattillo JM, Yazejian B, DiGregorio DA, Vergara JL, Grinnell AD, Meriney SD (2001) Contribution of pre-synaptic calcium-activated potassium currents to transmitter release regulation in cultured *Xenopus* nerve-muscle synapses. Neuroscience 102:229–240.

Ramanathan K, Michael TH, Jiang GJ, Hiel H, Fuchs PA (1999) A molecular mechanism for electrical tuning of cochlear hair cells. Science 283:215–217.

Roberts WM, Jacobs RA, Hudspeth AJ (1990) Colocalization of ion channels involved in frequency selectivity and synaptic transmission at presynaptic active zones of hair cells. J Neurosci 10:3664–3684.

Robitaille R, Garcia ML, Kaczorowski GJ, Charlton MP (1993) Functional colocalization of calcium and calcium-gated potassium channels in control of transmitter release. Neuron 11:645–655.

Rosenblatt KP, Sun ZP, Heller S, Hudspeth AJ (1997) Distribution of Ca^{2+}-activated K^+ channel isoforms along the tonotopic gradient of the chicken's cochlea. Neuron 19:1061–1075.

Rüttiger L, Sausbier M, Zimmermann U, Winter H, Braig C, Engel J, Knirsch M, Arntz C, Langer P, Hirt B, Muller M, Kopschall I, Pfister M, Munkner S, Rohbock K, Pfaff I, Rusch A, Ruth P, Knipper M (2004) Deletion of the Ca^{2+}-activated potassium (BK) {alpha}-

subunit but not the BK{beta}1-subunit leads to progressive hearing loss. Proc Natl Acad Sci USA 101:12922–12927.

Skinner L, Enée V, Beurg M, Hak Hyun J, Ryan AF, Hafidi A, Aran JM, Dulon D (2003) Contribution of BK Ca^{2+}-activated K^{+} channels to auditory neurotransmission in the guinea pig cochlea. J Neurophysiol 90:320–332.

Schopperle WM, Holmqvist MH, Zhou Y, Wang J, Wang Z, Griffith LC, Keselman I, Kusinitz F, Dagan D, Levitan IB (1998) Slob, a novel protein that interacts with the Slowpoke calcium-dependent potassium channel. Neuron 20:565–573.

Sobkowicz HM (1992) The development of innervation in the organ of Corti. In: Development of auditory and vestibular systems 2 (Romand R, ed), pp 59–95. Amsterdam: Elsevier Science Publishers BV.

Vergara C, Latorre R, Marion NV, Adelman JP (1998) Calcium-activated potassium channels. Curr Opin Neurobiol 8:321–329.

Waka N, Langer P, Rusch A, Mcenery MW, Platzer J, Striessnig J, Engel J (2003) Extrasynaptic colocalization of and interaction between Cav1.3 and BK channels in mouse inner hair cells. Abstract 814 ARO 2003.

Xia X, Hirschberg B, Smolik S, Forte M, Adelman JP (1998) dSLo interacting protein 1, a novel protein that interacts with large-conductance calcium-activated potassium channels. J Neurosci 18:2360–2369.

(Accepted 11 September 2004)
(Available online 11 November 2004)